

HT Camelopardalis: The simplest intermediate polar spin pulse

P.A. Evans^{*} and Coel Hellier

Astrophysics Group, School of Chemistry and Physics, Keele University, Staffordshire, ST5 5BG

Accepted Received

ABSTRACT

The intermediate polar HT Cam is unusual in that it shows no evidence for dense absorption in its spectrum. We analyse an *XMM-Newton* observation of this star, which confirms the absence of absorption and shows that the X-ray spin-pulse is energy independent. The modulation arises solely from occultation effects and can be reproduced by a simple geometrical model in which the lower accretion footprint is fainter than the upper one.

We suggest that the lack of opacity in the accretion columns of HT Cam, and also of EX Hya and V1025 Cen, results from a low accretion rate owing to their being below the cataclysmic variable period gap.

Key words: accretion, accretion discs – stars: individual: HT Cam (RX J0757.0+6306) – novae, cataclysmic variables – X-rays: binaries.

1 INTRODUCTION

A characteristic feature of intermediate polars (IPs) – interacting white-dwarf/red-dwarf binaries with a magnetic primary – is that their X-ray emission shows a clear modulation at the white-dwarf spin period (see Patterson 1994 for an overview of these objects).

Understanding these pulsations, however, is not straight forward since many factors can contribute to the modulation. These include opacity in the X-ray emitting accretion regions, and opacity owing to infalling material if it passes through the line of sight. Further, they include occultation as the accretion regions pass over the white-dwarf limb, including the effect of possible asymmetries between the two accreting poles. Thus IP spin pulses can show complex profiles, as exemplified by FO Aqr (e.g. Beardmore et al. 1998) and PQ Gem (e.g. Mason 1997).

It is thus useful to study systems where we can understand the pulse profile in terms of simple geometry alone. One such IP is XY Ari, where an eclipse provides geometrical information (Hellier 1997). Recent work on HT Cam suggests that it has an unusually simple spin pulse, since there appears to be very little opacity affecting the X-ray emission (de Martino et al. 2005), and thus no complications owing to absorption by accretion curtains.

In this paper we analyse *XMM* data on HT Cam and produce a geometric model of the pulse, leading to constraints on the accretion geometry in this system.

2 OBSERVATIONS

HT Camelopardalis (RX J0757.0+6306, hereafter HT Cam) was observed by the *XMM-Newton* satellite (Jansen et al. 2001) for ~ 40 ks on 2003 March 24. AAVSO data reveal that the system was quiescent at $V \sim 17$. The EPIC MOS (Turner et al. 2001) and PN (Strüder et al. 2001) instruments were operating in FULL FRAME MODE, observing through the Medium filter. Data from these three instruments were extracted from circular regions of radius 14 arc sec, centred on the source. An annulus around this was used to estimate the background. The OM camera (Mason et al. 2001) was also in operation, collecting 17.5 ks of data through each of the *B* and *UVW2* filters. The data were analysed using the *XMM-SAS* software, v6.0.0.

The lightcurves are shown in Fig. 1. The X-ray data show clear modulation at the 515-s white-dwarf spin period. Fourier analysis confirms the spin pulse but shows no orbital or beat modulation. In the *B* band there is a ~ 5 per cent spin-period modulation, but there is no detectable pulse in the UV-band, up to a limit of ~ 14 per cent. The mean X-ray count-rate in the pn detector is 1.05 counts s⁻¹, which corresponds to a 0.2–12 keV flux of 6.5×10^{-12} erg cm⁻² s⁻¹; for comparison the 0.1–2.4 keV flux observed by *ROSAT* was 1.87×10^{-12} erg cm⁻² s⁻¹ (Tovmassian et al. 1998).

3 SPECTROSCOPY

X-ray emission in an IP comes from multi-temperature plasmas beneath the accretion shock. To model the spectrum of HT Cam we used MEKAL components in XSPEC, absorbed by

^{*} pae@astro.keele.ac.uk

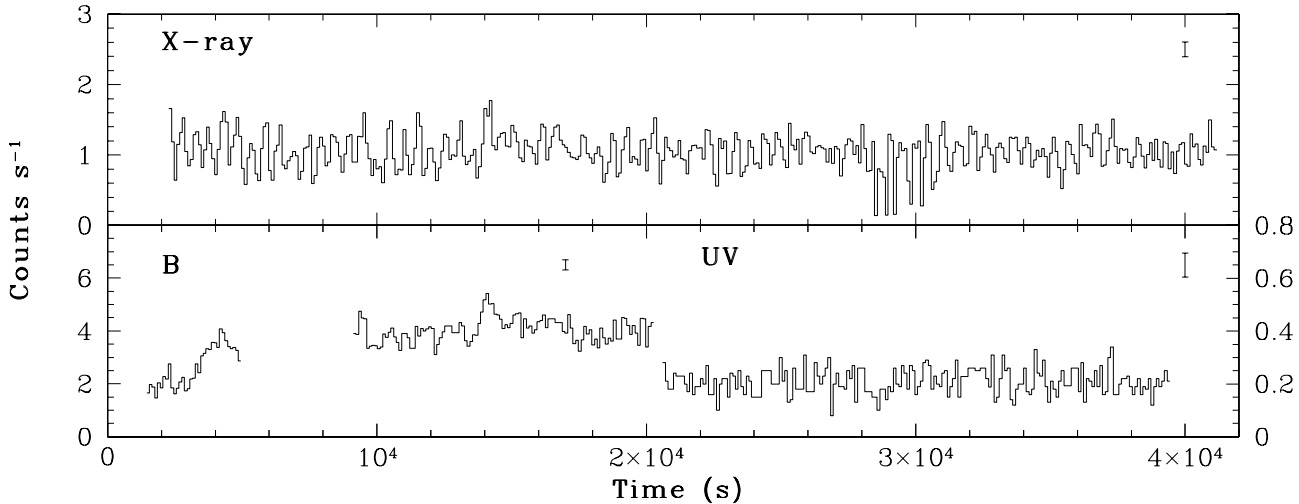


Figure 1. Lightcurves of HT Cam in the X-ray (EPIC-pn; 0.2–12 keV), B (3900–4900 Å) and UV (1800–2250 Å) bands. The bins are 100 s, and the 515-s spin-pulse can be clearly seen in the X-ray band. Typical errors are shown.

both simple and partial covering absorption. To reduce the effects of cross-calibration uncertainties the MEKAL normalisations were permitted to optimise independently for the three EPIC instruments. All other parameters were kept the same for the three detectors. Using two MEKALs of different temperatures gave a χ^2 of 1530 ($\chi^2_\nu=1.20$); adding a third MEKAL reduced χ^2 to 1428 ($\chi^2_\nu=1.12$), and a fourth gave a χ^2 of 1331 ($\chi^2_\nu=1.05$). The addition of a fifth MEKAL did not improve the fit.

The CEMEKL model in XSPEC reproduces MEKAL emission along a continuous range of temperatures, where normalisation varies according to $(T/T_{\text{MAX}})^\alpha$. We tried replacing our four discrete MEKALs with a CEMEKL, but this worsened the fit to a χ^2 of 1385 ($\chi^2_\nu=1.08$).

In all of the above fits, the column density of the partial absorber tended to zero. We thus removed it, with no affect on the fit quality. We also tried adding a soft blackbody component, as is seen in some IPs (e.g. de Martino et al. 2004) but this gave almost no improvement in fit quality ($\Delta\chi^2 \sim 4$). The EPIC-pn spectrum plus the four-MEKAL model are shown in Fig. 2, and the parameters for the model are given in Table 1. Note that, as the parameters are expected to vary on the spin cycle, these may be weighted averages.

4 THE SPIN PULSE

The spin-pulse profile of HT Cam is shown in Fig. 3. We can describe the X-ray pulse as a flat maximum covering phases ~ 0.7 – 1.1 and a dip covering ~ 0.2 – 0.6 . To investigate the cause of this dip we extracted spectra from the two phase regions and fitted the four-MEKAL model to both simultaneously. Initially we allowed all parameters to vary between the two regions, which gave a χ^2 of 1750 ($\chi^2_\nu=1.04$). This was almost unchanged ($\chi^2=1753$, $\chi^2_\nu=1.04$) if the absorption was tied between the regions. We tried adding a partial absorber to the phase-minimum spectrum, but it made no difference to the fit, with the column density tending to zero. As a check we tried forcing the emission to remain constant

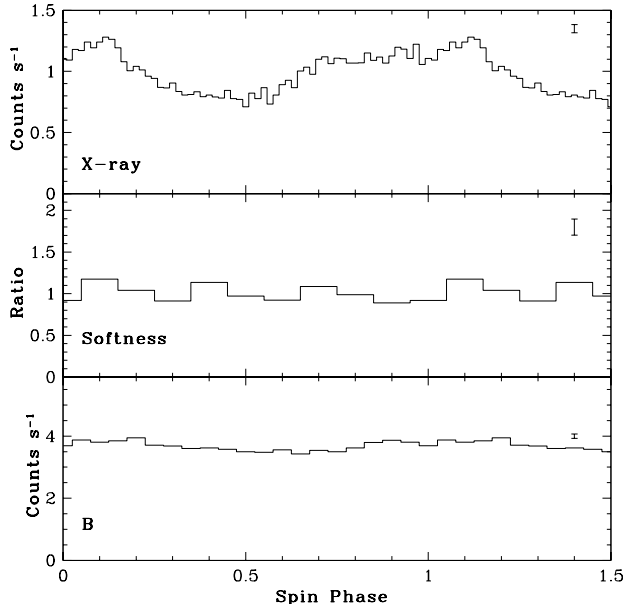


Figure 3. The spin pulse-profile of HT Cam, with typical errors. The upper panel shows the mean 0.2–12 keV flux from all three EPIC cameras. The softness ratio is defined as $(0.2–4)/(6–12)$ keV. The B band is as Fig. 1. Phase zero is defined from the ephemeris of Kemp et al. (2002).

across spin-phase, varying only the absorption. This gave a poor fit ($\chi^2=1969$, $\chi^2_\nu=1.15$). We thus conclude that the spin-pulse is not caused by absorption variations, but must result from variations in the underlying X-ray emission.

The softness ratio shows almost no modulation on the spin-period, implying that the modulation is energy-independent. We thus fixed the absorption and the ratios of the emission components across spin phase, attempting to reproduce the observed spectral changes by reducing the flux during the dip but keeping the ‘colour’ constant. This gave a good fit ($\chi^2=1780$, $\chi^2_\nu=1.05$) which suggests that

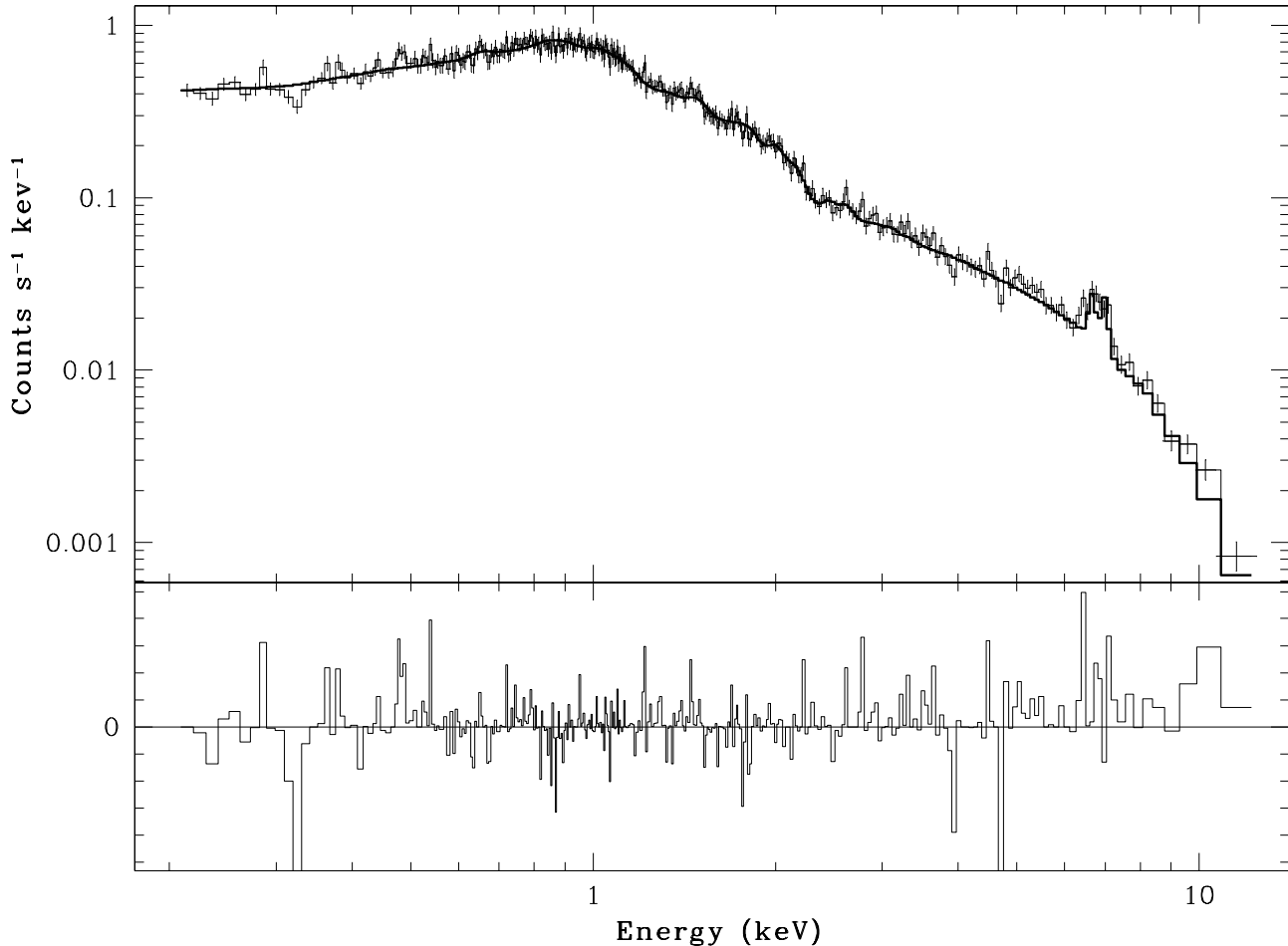


Figure 2. The EPIC-pn spectrum of HT Cam, fitted by a four-MEKAL model (see text). Note the prominence of the thermal Iron-K emission complex around 6.7 keV. The residuals provide evidence for a 6.4-keV component of cold iron, having an equivalent width of 70 eV.

the modulation is indeed energy independent within *XMM*'s pass-band.

In an IP the accretion disc is magnetically truncated, with material flowing along the magnetic field lines in large 'accretion curtains'. In many systems these curtains periodically pass through our line of sight, causing a prominent absorption dip (e.g. AO Psc, Hellier, Cropper & Mason 1991; FO Aqr, Beardmore et al. 1998; V1223 Sgr, Taylor et al. 1997). The low absorption in our spectroscopy and the energy-independent nature of the spin-pulse mean that this cannot be happening in HT Cam. Further, they suggest that the post-shock accretion columns themselves have an unusually low opacity, so that we see no difference in the spectra when viewing them at different angles. This contrasts with, for example, V405 Aur, where the accretion curtains never cross our line of sight, but the changing aspect of the columns themselves gives hardness-ratio changes on the spin-period (Evans & Hellier 2004).

We suggest that, in contrast, the spin pulse in HT Cam arises solely from simple occultation effects as the accretion columns pass over the white-dwarf limb as it rotates. This allows us to investigate the X-ray spin pulse with a simple geometrical model.

5 MODELLING THE EFFECTS OF OCCULTATION

We constructed a model which consists of arc-shaped accretion regions of zero height above the white-dwarf surface (since the majority of the X-ray emission in an IP occurs close to the white-dwarf surface, see Cropper, Wu & Ramsay 2000). The shape and location of the arcs was determined by assuming a disc disrupted at r_{mag} , and by tracing field lines from there to the white-dwarf surface, assuming a magnetic dipole inclined to the spin axis by an angle δ and offset from the white-dwarf centre in an arbitrary direction. A schematic diagram of this model is shown in Fig. 4. Since accretion rate will likely vary with azimuth, being greatest at the point to which the magnetic pole points, we assume a brightness varying as

$$B(\gamma) = A \cos^2 \left(\frac{\pi \gamma}{2\Delta\gamma} \right) \quad (1)$$

where γ is the magnetic longitude of a point on the footprint, between end-points $\pm\Delta\gamma$, and A is a brightness coefficient, which can take different values for the upper and lower regions. By default the upper accretion lay between $\pm 90^\circ$ and the lower one covered 90 – 270° . The star was then rotated

Component	Parameter (Units)	Value	Error
Absn.	n_{H} (cm $^{-2}$)	5.35×10^{20}	(+0.28, -0.45)
Mekal	kT (keV)	0.172	(+0.029, -0.033)
	Abundance	0.622	(+0.103, -0.104)
	Norm (M1)	4.11×10^{-5}	(+8.05, -4.11)
	Norm (M2)	7.63×10^{-5}	(+9.94, -4.67)
	Norm (PN)	1.02×10^{-4}	(+6.24, -3.32)
Mekal	kT (keV)	0.678	(+0.022, -0.022)
	Norm (M1)	1.52×10^{-4}	(+0.33, -2.67)
	Norm (M2)	1.46×10^{-4}	(+0.32, -2.54)
	Norm (PN)	1.97×10^{-4}	(+6.53, -0.14)
Mekal	kT (keV)	1.99	(+0.29, -0.26)
	Norm (M1)	5.45×10^{-4}	(+1.69, -2.09)
	Norm (M2)	6.88×10^{-4}	(+0.93, -1.72)
	Norm (PN)	5.59×10^{-4}	(+1.38, -1.33)
Mekal	kT (keV)	13.4	(+2.6, -2.1)
	Norm (M1)	2.25×10^{-3}	(+0.67, -0.16)
	Norm (M2)	2.00×10^{-3}	(+0.17, -0.10)
	Norm (PN)	2.06×10^{-3}	(+8.23, -0.12)

Table 1. Model components and parameters fitted to the phase-averaged spectrum of HT Cam (see Section 3). The errors are given to the same power of ten as the values.

through one revolution in 100 phase bins and a simulated pulse-profile was produced by summing the brightness of the visible emitting regions. We ignored projection effects, treating the X-ray emission as optically thin.

Some form of asymmetry between the two accretion regions is necessary to produce any modulation, otherwise the occultation of the upper pole is compensated for by the emergence of the lower pole. We explored three sources of asymmetry: offsets of the dipole in different directions; reducing the azimuthal extent of one region compared to the other; and reducing the brightness of one region compared to the other. We explored these asymmetries over a full range of system inclination (i) and the dipole inclination (δ), in steps of 10° .

A selection of model pulse-profiles is given in Fig. 5 and discussed below. Note that if we reverse the sense of the asymmetry between the poles, the pulse-profiles are inverted.

5.1 Offsetting the dipole

We first offset the dipole along the x -axis (perpendicular to the plane of the spin and magnetic axes, see Fig. 4). Since disappearance of one pole is not coincident with appearance of the other, there is a modulation. However it is very different from the data (Fig. 5, top row), so is not considered further.

If the offset is instead in the y -direction (in the plane of the spin and magnetic axes), the lower footprint will not appear over the limb at all when i and δ are low. This results in a deep dip (Fig. 5, second row). The flux seen at minimum in Fig. 5 results because the upper pole is never totally occulted. When i and δ are higher the lower footprint does appear, but not until after the upper one has begun to be occulted, hence a partial dip is seen. Once the

lower pole does appear it causes the flux to rise, causing a ‘hump’ during the dip.

Invoking a z -offset (i.e. along the spin axis) makes the magnetic latitude of the footprints bigger at one pole than the other. At low values of i and δ this prevents the lower footprint from ever being seen (Fig. 5, third row). As i and δ increase, the lower footprint does appear, but as it is smaller than the upper one it appears and disappears more rapidly, which gives rise to a ‘hump’.

None of the above offsets result in a pulse profile resembling that in HT Cam.

5.2 Reducing the size of the lower pole

We tried reducing the longitudinal range of the lower arc, keeping the brightness coefficient (A) the same, so that the lower pole becomes fainter overall. The difference in total brightness between the poles gives rise to a dip. The mid-part of ingress is flat, since appearance of one pole is cancelling with disappearance of the other. However, the effect of the smaller footprint is confined more to the middle of the ingress, so a decline is seen at the beginning and end of ingress.

In the above the total brightness of the lower footprint is less than that of the upper. We have explored, instead, changing the brightness coefficient such that the total brightnesses are the same. This gives a worse match to the data, with a ‘hump’ being seen instead of a dip, and is not shown in Fig. 5.

Again, the asymmetries considered in this section do not produce profiles like that seen in HT Cam.

5.3 Making the lower footprint fainter

Keeping the dipole symmetrical, but reducing the brightness coefficient for the lower footprint, results in a smooth modulation as the upper footprint is progressively replaced with the fainter lower one (Fig. 5, bottom row). Changing the system and dipole inclinations alters the width and profile of the dip. If δ and i are high the entire lower pole is visible for some time, producing a flat-bottomed minimum.

This model gives the only good match to the data. Good fits can be found for a system inclination of $\sim 40\text{--}70^\circ$, and a dipole inclination of $\sim 20\text{--}50^\circ$. Here the footprints lie between $\pm 90^\circ$ (upper) and $90\text{--}270^\circ$ (lower). To reproduce the depth of the dip the lower footprint is 65 per cent as bright as the upper one. The magnetic latitude of these regions corresponds to a magnetospheric radius of $\sim 1.3\text{--}3.6 R_{\text{WD}}$. Fig. 6 shows the system with the best-fitting parameters ($i = 55^\circ$, $\delta = 35^\circ$, $R_{\text{mag}} = 2.6 R_{\text{WD}}$) and shows that the accretion curtains do not intersect our line of sight in this geometry, as required by the lack of absorption in the spectra.

6 DISCUSSION

We have found there to be little evidence for opacity in the X-ray spectrum of HT Cam, suggesting that the spin pulse must result solely from geometric effects. We have thus produced model pulse profiles for a range of possible geometries. We find that only one matches the data, namely one in which the lower accretion region is fainter than the upper one. By

fine-tuning this model to the data we find that the inclination of HT Cam is $\sim 55^\circ$, while the magnetic dipole makes an angle of $\sim 35^\circ$ to the spin axis (see Fig. 6).

Analysis of an *XMM-Newton* observation of HT Cam has shown the pulse-profile to be energy-independent. By creating model pulse-profiles we show that this can be explained by the upper pole being periodically occulted by the white-dwarf, provided that the lower accretion region is fainter than the upper one. Our models also suggest that the inclination of HT Cam is $\sim 55^\circ$, while the magnetic dipole makes an angle of $\sim 35^\circ$ to the spin axis.

The energy independent nature of the X-ray spin-pulse in HT Cam and the lack of absorption in its spectrum is unusual, since most IPs show spectral variations over the spin cycle and prominent, phase-varying absorption. One part of the explanation is that, in HT Cam, the accretion curtains do not cross our line-of-sight to the X-ray emitting regions. But this alone is not sufficient to explain the energy-independent X-ray modulation: Evans & Hellier (2004) and de Martino et al. (2004) report that the same is true in V405 Aur, however the pulse profile of that star is energy dependent. In that system, the energy dependence is thought to arise from opacity within the accretion columns, which changes with the viewing angle.

The fact that we don't see this in HT Cam suggests that the opacity in the accretion column is low. Only two other IPs are known in which a dense absorber ($n_H > 2 \times 10^{21} \text{ cm}^{-2}$) is not needed to fit the X-ray spectrum, namely EX Hya and V1025 Cen (see Allan, Hellier & Beardmore 1998 and Hellier, Beardmore & Buckley 1998, respectively). Like HT Cam, these system both lie below the period gap, where systems are believed to have accretion rates an order of magnitude lower than those above the gap (e.g. Warner 1987).

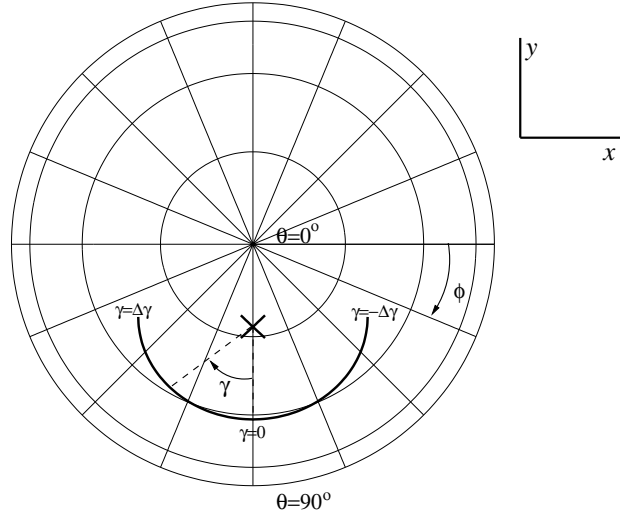
Mukai et al. (2003) came to a similar conclusion for EX Hya. They analysed *Chandra* HETG spectra of several IPs above the gap and also of EX Hya. They found much more line emission in the latter, which they attributed to an optically thin accretion column, probably resulting from a low specific accretion rate.

We thus suggest that the X-ray spectra of IPs depend on whether they are above or below the cataclysmic variable period gap. Those above the period gap have high accretion rates, resulting in optically thick accretion columns and prominent phase-varying absorption when accretion curtains obscure the line of sight. Those below the gap have much lower accretion rates, optically thin accretion columns and show much less absorption in their spectra.

ACKNOWLEDGEMENTS

We thank Sean Harmer for his help during this analysis.

REFERENCES



de Martino D., Matt G., Mukai K., Bonnet-Bidaud J.M., Gänsicke B.T., Haberl F., Mouchet M., 2005, in Hameury J.M., Lasota J.P., eds, ASP Conf. Ser Vol. 330, The astrophysics of cataclysmic variables and related objects, Astron. Soc. Pac., San Francisco, p. 403

Evans P.A., Hellier C., 2004, MNRAS, 353, 447

Hellier C., 1997, MNRAS, 291, 71

Hellier C., Cropper M., Mason K.O., 1991, MNRAS, 248, 233

Hellier C., Beardmore A.P., Buckley D.A.H., 1998, MNRAS, 299, 851

Jansen F. et al., 2001, A&A, L1

Kemp J., Patterson J., Thorstensen J.R., Fried R.E., Skillman D., Billings G., 2002, PASP, 114, 623

Mason K.O., 1997, MNRAS, 285, 493

Mason K.O., et al., 2001, A&A, 365, L36

Mukai K., Kinkhabwala A., Peterson J.R., Kahn S.M., Paerels F., 2003, ApJ, 586, L77

Patterson J., 1994, PASP, 106, 209

Strüder L. et al., 2001, A&A, 365, L18

Taylor P., Beardmore A.P., Norton A.J., Osborne J.P., Watson M.G., 1997, MNRAS, 289, 349

Tovmassian G.H., et al., 1998, A&A, 335, 227

Turner M.J.L. et al., 2001, A&A, 365, L27

Warner B., 1987, MNRAS, 227, 23

Allan A., Hellier C., Beardmore A.P., 1998, MNRAS, 295, 167

Beardmore A.P., Mukai K., Norton A.J., Osborne J.P., Hellier C., 1998, MNRAS, 297, 337

Cropper M., Wu K., Ramsay G., 2000, NewAR, 44, 57

de Martino D., Matt G., Belloni T., Haberl F., Mukai K., 2004, A&A, 415, 1009

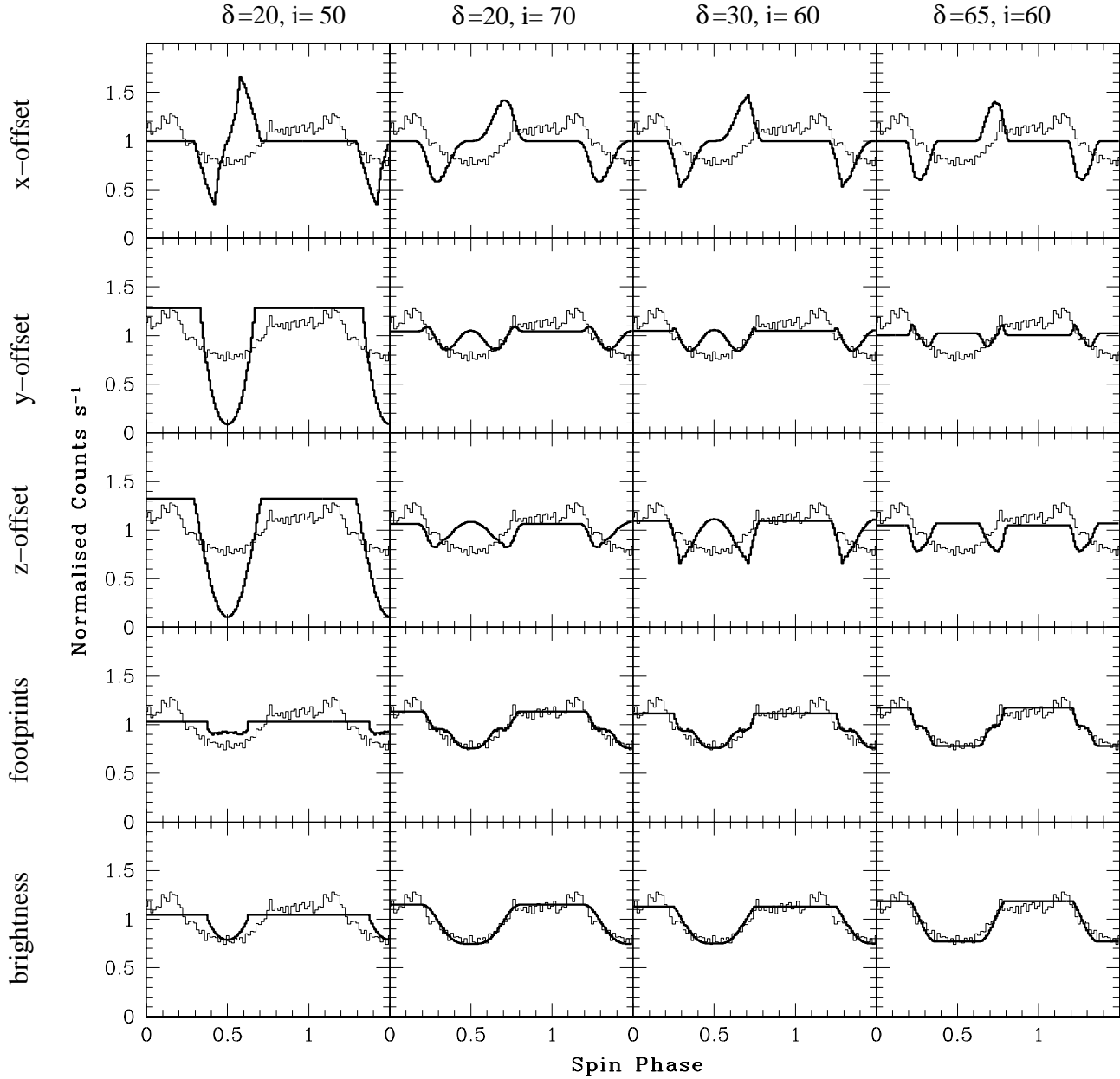


Figure 5. Simulated X-ray pulse profiles. In the upper rows the dipole is offset by 0.15 R_{WD} in the x , y - and z directions. The upper footprint covers $-90^\circ \leq \gamma \leq 90^\circ$ and the lower ones covers $90^\circ \leq \gamma \leq 270^\circ$ in all but the ‘footprints’ row. Here the lower footprint covers $120^\circ \leq \gamma \leq 240^\circ$. In the bottom row the lower footprint is 65 per cent as bright as the upper one.

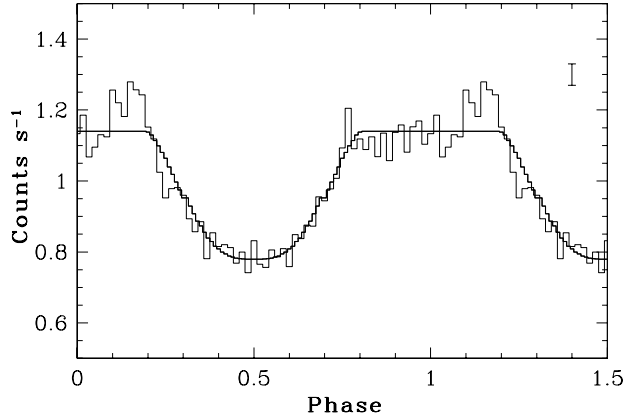


Figure 6. The best-fitting model, as described in the text. *Left panel:* The data and model lightcurve. *Right panel:* A schematic view of the system. The upper and lower accretion curtains are shown as dashed and dotted lines respectively, while the ring shows the inner edge of the disc. We can see that the accretion curtains never cross our line of sight to the footprints.